Trajectory and CubeSat Mission Design for Plasma Physics Observations during the 2029 Apophis Flyby

9th IAA Planetary Defense Conference 2025 - Student Competition

Lucas Barbero Sánchez, Emil Vinterhav, Stas Barabash

***Abstract*—On April 13th 2029, Apophis, a 400-meter asteroid will pass within 31 600 km of Earth's surface in a retrograde orbit, moving through the magnetosphere and encountering the outer radiation belt, ring current, and outer edges of the plasmasphere. Therefore, this rare event offers a fantastic opportunity to investigate how small scale airless bodies interact with Earth's magnetosphere. This paper proposes an initial trajectory concept for a CubeSat mission with the objective of conducting plasma and neutral gas measurements during the Apophis flyby. The main focus of this work is the design and optimization of the spacecraft trajectory, using a combination of a Weak Stability Boundary (WSB) transfer and an electric thrust propulsion phase.**

I. Introduction

Apophis' close flyby on April 13th 2029 offers a unique opportunity for space plasma physics [1]. The asteroid will pass within 31,600 km of Earth's surface in a retrograde orbit, moving through the magnetosphere and encountering the outer radiation belt, ring current, and outer edges of the plasmasphere. As it moves through these regions, particle interactions may release ions and neutrals, revealing surface composition and influencing levitating dust dynamics. To investigate these effects, a CubeSat equipped with plasma and neutral gas analyzers could provide valuable measurements during this encounter.

Consequently, the concept arises of designing a low-thrust electric propulsion mission capable of intercepting Apophis and flying alongside it for a few hundred minutes. However, designing a viable trajectory for such a mission presents significant challenges, particularly given Apophis' velocity of 7.42 km/s relative to Earth at close approach.

One interesting approach is through a Weak Stability Boundary (WSB) maneuver. The WSB is a region that enables efficient transfers, as objects in it are not strongly gravitationally bound to anything. This is particularly interesting because it implies that small perturbations can lead to huge orbit changes. This characteristic makes WSB transfers particularly efficient and flexible in terms of time window availability. This concept was first utilized by the Hiten spacecraft [2] in 1991, allowing for an extremely low-cost ΔV lunar capture.

In this context, an intriguing question arises: could a WSB maneuver lead to a flexible and rapid enough transfer to successfully intercept Apophis during its closest approach? This work provides an initial exploration of this possibility by studying the Circular Restricted Three-Body Problem (CR3BP), periodic orbits around Lagrange points, invariant manifolds, and the transfer problem.

II. The Circular Restricted Three Body Problem

A. Non-dimensionalization

Before diving into the CR3BP, it is convenient to first non-dimensionalize the relevant quantities: mass, distance, and time. The following definitions are traditionally used:

$$M^* = m_1 + m_2 \tag{1}$$

$$L^* = l_1 + l_2 \tag{2}$$

$$T^* = \sqrt{\frac{{L^*}^3}{GM^*}} \tag{3}$$

Where m_1 and m_2 are the masses of the two primary bodies, l_1 and l_2 their distances from barycenter, and T^* the period or characteristic time, as given by Kepler's third law.

B. Equations of Motion

In the context of the N-body problem, the system's dynamics are classically governed by Newton's law of gravitation:

$$\ddot{\vec{r}}_i = -G \sum_{j \neq i}^{N} \frac{m_j}{r_{ji}^3} \vec{r}_{ji} \tag{4}$$

Even when $N = 3$, there is no analytical solution for eqn. 4. Therefore, for practical purposes, the system's dynamics are simplified under the following conditions.

- The mass of the tertiary object (spacecraft) is extremely small compared to m_1 (Sun) and m_2 (Earth).
- The mass m_1 is greater than m_2 and $\mu \equiv m_2/M^*$.
- The two primary objects follow circular orbits around their barycenter.

This is known as the Circular Restricted Three-Body Problem (CR3BP). In the rotating coordinate system, the origin is placed at the system's barycenter, and the x-axis is aligned along the line connecting the two primary bodies, m_1 and m_2. The y-axis is perpendicular to the x-axis in the plane of motion, and the z-axis is perpendicular to the orbital plane.

This coordinate system simplifies the study of the system's dynamics by focusing on the motion of a third body (such as a spacecraft) relative to the two primary bodies.

In the rotating coordinate system, the equations of motion, as derived from [3], describe the motion of a small body (the spacecraft) under the gravitational influence of the two primary bodies, m_1 and m_2.

These equations are:

$$\ddot{x} - 2\dot{y} - x = -\frac{(1-\mu)(x+\mu)}{d^3} - \frac{\mu(x-(1-\mu))}{r^3} \tag{5}$$

$$\ddot{y} + 2\dot{x} - y = -\frac{(1-\mu)y}{d^3} - \frac{\mu y}{r^3} \tag{6}$$

$$\ddot{z} = -\frac{(1-\mu)z}{d^3} - \frac{\mu z}{r^3} \tag{7}$$

where d and r are the distances to the primary and secondary bodies, respectively, given by:

$$d = \sqrt{(x+\mu)^2 + y^2 + z^2} \tag{8}$$

$$r = \sqrt{(x-1+\mu)^2 + y^2 + z^2} \tag{9}$$

However, these equations can be expressed more compactly through the definition of an effective potential function:

$$U = \frac{1}{2}(x^2 + y^2) + \frac{(1-\mu)}{d} + \frac{\mu}{r} \tag{10}$$

such that

$$\ddot{x} - 2\dot{y} = U_x \tag{11}$$

$$\ddot{y} + 2\dot{x} = U_y \tag{12}$$

$$\ddot{z} = U_z \tag{13}$$

where the subscript denotes the partial derivative of U with respect to the corresponding coordinate.

One can also define the Jacobi Integral, which is the only constant of motion in the CR3BP. This can be formulated as:

$$C_J = 2U - (\dot{x}^2 + \dot{y}^2 + \dot{z}^2) \tag{14}$$

This function is interesting because it determines the regions of space that the small body can and cannot enter.

C. Lagrange Points

There are five equilibrium points in the CR3BP where $\nabla U = 0$, meaning that the gravitational forces of the two primary bodies and the centrifugal force balance each other. Among these points, L_1 and L_2 are particularly interesting because they are collinear with Earth and relatively close to it, and because periodic orbits exist around them. The idea is to initiate the transfer from one of these periodic orbits.

The location of these points depends on μ, which, for this particular case, was defined taking the Moon into account, $m_2 = m_{\text{E}} + m_{\text{M}}$. This approach was deemed more realistic.

Table I: Location for Lagrange points in the Sun-Earth system, and the C_J for each one.

L_i	x	y	z	C_J
L_1	0.989986	0	0	3.0008979
L_2	1.010075	0	0	3.0008938
L_3	-1.010078	0	0	3.0003056
L_4	0.499997	0.866025	0	2.9999969
L_5	0.499997	-0.866025	0	2.9999969

III. Differential Corrector Algorithm

The departure for our transfer to Apophis will be from a periodic orbit around either L_1 or L_2. However, finding these orbits is not trivial. This section develops a differential corrector algorithm, following a similar approach to [4] and [5], requiring the linearized equations of motion and the state transition matrix.

A. Linearized Equations of Motion

The equations of motion can be linearized around the equilibrium points, shown in Table I, by introducing a small perturbation, $r_{i,j} = r_{L_j} + \eta_i$ and retaining only the first-order terms of the Taylor expansion of U, leading to:

$$\ddot{\xi} - 2\dot{\eta} = U_{xx}\ \xi + U_{xy}\ \eta \tag{15}$$

$$\ddot{\eta} + 2\dot{\xi} = U_{yx}\ \xi + U_{yy}\ \eta \tag{16}$$

$$\ddot{\zeta} = U_{zz}\ \zeta \tag{17}$$

Consequently, the linearized system takes the following form:

$$\dot{\vec{s}}(t) = A(t)\ \vec{s}(t) \tag{18}$$

where the state vector is defined as $\vec{s} = [x, y, z, \dot{x}, \dot{y}, \dot{z}]$ and $A(t)$ denotes the system's Jacobian.

$$A(t) = \begin{pmatrix} 0 & 0 & 0 & 1 & 0 & 0 \\ 0 & 0 & 0 & 0 & 1 & 0 \\ 0 & 0 & 0 & 0 & 0 & 1 \\ U_{xx} & U_{xy} & U_{xz} & 0 & 2 & 0 \\ U_{yx} & U_{yy} & U_{yz} & -2 & 0 & 0 \\ U_{zx} & U_{zy} & U_{zz} & 0 & 0 & 0 \end{pmatrix} \tag{19}$$

B. The State Transition Matrix

The linearized equations of motion allow for the definition of the state transition matrix (STM), which governs the evolution of the system's Jacobian A, as defined in eqn.20 below.

$$\dot{\Phi}(t, t_0) = A(t)\ \Phi(t_0)\ , \qquad \Phi(t_0, t_0) = \mathbf{I}_{6\times 6} \tag{20}$$

This implies that the system's evolution over time can be described using the STM, such that:

$$\vec{s}(t) = \Phi(t, t_0)\ \vec{s}(t_0) \tag{21}$$

where $[\Phi]_{i,j}(t) = \frac{\partial r_i(t)}{\partial \dot{r}_j(t_0)}$ denotes the $\{i, j\}$ STM's element.

Lastly, the monodromy matrix is defined as the STM evaluated over one full period of a periodic orbit, such that:

$$M = \Phi(T, t_0) \tag{22}$$

The monodromy matrix will be crucial in generating the Lyapunov and Halo families of orbits.

C. Lyapunov Orbits

Lyapunov orbits are defined as planar periodic orbits around either L_1 or L_2, and have the property of being symmetric with respect to the $y = 0$ plane. Conveniently, this eliminates time as a variable, as the trajectory is propagated until a crossing occurs.

The idea behind the differential corrector algorithm is simple: given a sufficiently good initial guess, the algorithm uses a shooting method to the $y = 0$ plane (half a period), computes the error and iteratively refines the initial condition until the error falls within a desired tolerance.

One good guess is an initial condition of the form:

$$\vec{s}_0 = \begin{bmatrix} x_0 & 0 & 0 & 0 & \dot{y}_0 & 0 \end{bmatrix}^T \tag{23}$$

Then, following eqn. 21, the initial condition is iteratively refined using:

$$\dot{y}^*(t_0) = \dot{y}(t_0) - \left[\frac{\partial \dot{x}(t_{T/2})}{\partial \dot{y}(t_0)}\right]^{-1} \cdot e \tag{24}$$

Once the error magnitude falls within the desired tolerance, the complete orbit is obtained by integrating over $t \in [T/2, T]$.

The rest of the Lyapunov orbit family can be computed through continuation, which consists of slightly perturbing x_0 and using the initial condition from the previous orbit. These are all potential candidate departure orbits from where a WSB transfer could be initiated. Some of these are shown in Figure 1 below, along with Apophis' trajectory in the rotating coordinate frame. The asteroid's ephemeris was taken from the JPL Small-Body Database [6] with respect to the SSB and then manually transformed into our coordinate system.

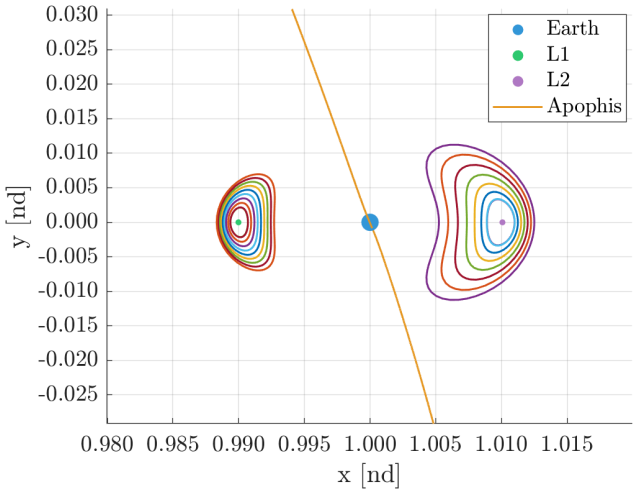

Figure 1: Lyapunov orbits around L_1 and L_2 in the Earth-Sun system, along with Apophis's trajectory in this frame. The Earth's size is exaggerated for visualization purposes, highlighting the asteroid's close approach. Naturally, and fortunately for us, Apophis's path does not intersect Earth's physical volume. All distances are non-dimensionalized.

D. Halo Orbits

Halo orbits are another example of periodic motion around L_1 and L_2, but in three dimensions, while still maintaining the symmetry of Lyapunov orbits with respect to the $y = 0$ plane. The method for determining them was similar to that one of Lyapunov orbits: starting with a sufficiently good initial guess, computing the error, and iteratively refining the initial condition until the error falls within the desired tolerance. However, in this case, the general form of the initial state vector included an additional component:

$$\vec{s}_0 = \begin{bmatrix} x_0 & 0 & z_0 & 0 & \dot{y}_0 & 0 \end{bmatrix}^T \tag{25}$$

In order to find a good initial guess for the computation of the first Halo orbit, it was necessary to identify the bifurcation orbit [7] from the Lyapunov family. The bifurcation orbit is a unique orbit that belongs to both the Lyapunov and Halo families. This is an orbit where the six eigenvalues of the monodromy matrix (the STM evaluated over one full period) have specific characteristics.

These eigenvalues can be grouped into three pairs:

- The first pair, consisting of a very large and a very small eigenvalue, is associated with the unstable and stable directions of the orbit, and is crucial for computing the invariant manifold.
- The second pair corresponds to the trivial eigenvalues, which are a result of time invariance or periodicity, and take the value 1.
- The final pair is associated with the vertical eigenmode.

The bifurcation orbit can be identified because its third pair of eigenvalues must equal 1. This enabled the determination of multiple northern and southern Halo orbits, which could serve as potential departure orbits for initiating a WSB transfer. Some of these are plotted in Figure 2 below.

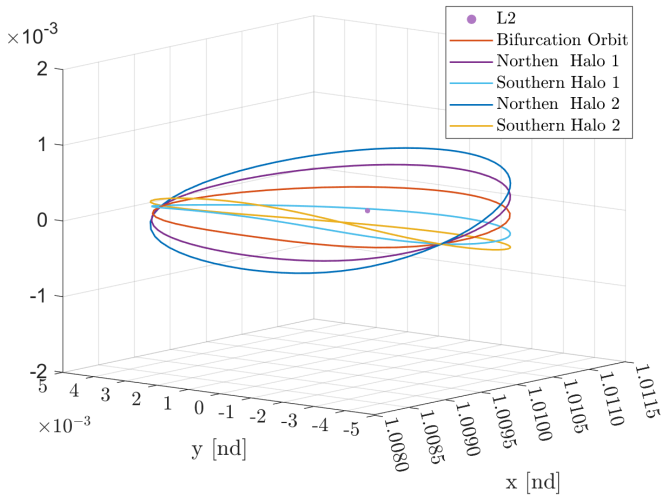

Figure 2: Halo orbits around L_2 in the Earth-Sun system.

IV. Trajectory Profile Idea

Lastly, it is time to bring all these concepts together. For simplicity, and since this is still a work in progress, we will select the bifurcation orbit around L_1 as the departure orbit from where to initiate the WSB transfer.

A small perturbation in the direction of the eigenvector associated with the largest eigenvalue of the STM (the unstable direction) caused the spacecraft to fall towards Earth. This is commonly referred to in the literature as a WSB transfer through the unstable invariant manifold [8] associated with the orbit. The total duration for the WSB maneuver shown in Figure 3 below was 17.4 days.

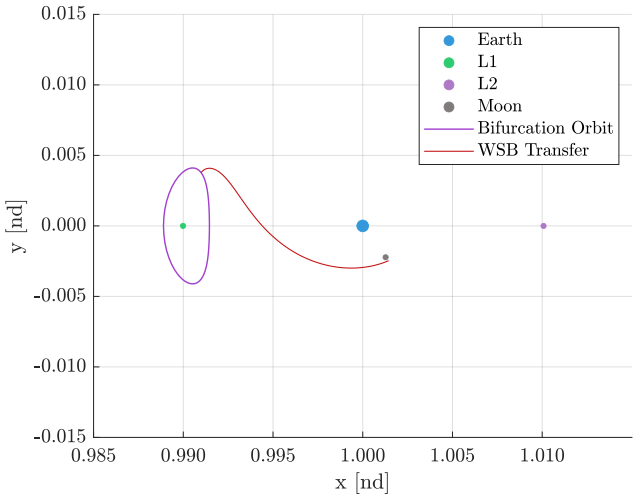

Figure 3: WSB maneuver initiated from the L_1 bifurcation orbit via the unstable invariant manifold.

The idea now is for the spacecraft to begin accelerating in order to escape the Earth-Moon system, with the goal of gaining velocity, rendezvousing, and intercepting Earth from behind, matching Apophis at close approach. Proper timing could provide an opportunity for a lunar gravity assist, giving the spacecraft an additional velocity boost as it departs from Earth. However, this effect was not modeled, as we focused only on the dynamics of the Sun-Earth system. Nevertheless, the Moon's ideal position was plotted in Figure 3 above, providing insight into how this could look.

Depending on the thrust direction, the characteristics of the propulsion system, and the spacecraft's total mass, many different outcomes might arise. The spacecraft's instrument payload was estimated to weigh 10 kg, as given in [1]. For this study, a propulsion system with characteristics similar to the JPT150-I2 Iodine Hall Thruster [9] was selected, leading to an estimated total spacecraft mass of 22.5 kg. This value was considered to be constant during this whole analysis.

Figure 4 shows the complete spacecraft trajectory. As the spacecraft accelerates, it gets away from the Earth, initially thrusting tangentially to its velocity and gradually adjusting the thrusting angle for the spacecraft to rendezvous with Apophis. After 321.6 days, the spacecraft reaches Apophis' position at closest approach with a velocity of 4.8 km/s, which is still significantly lower than Apophis' 7.4 km/s.

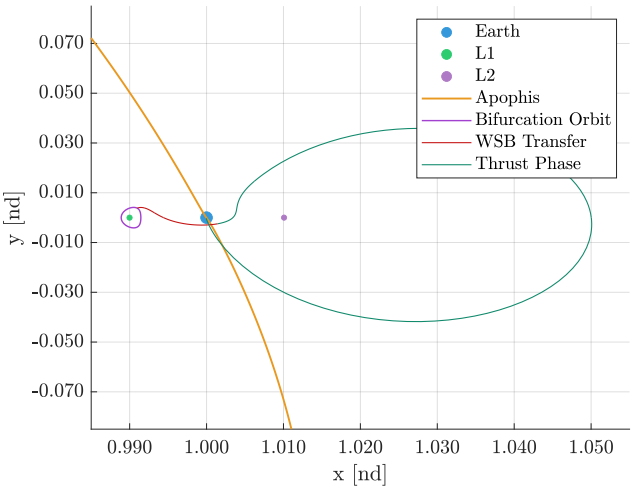

Figure 4: Spacecraft complete trajectory profile.

V. Conclusion

A trajectory profile was computed using a WSB transfer and a thrusting phase, intercepting Apophis during close approach with a velocity of 4.8 km/s. While this velocity is significantly lower than Apophis' 7.4 km/s, there is considerable room for improvement, as this is still a work in progress. Ongoing developments, such as exploring different departure orbits, refining the spacecraft's mass budget and thrusting capabilities, incorporating a more precise dynamical model (including the Moon's gravitational influence), and applying a more rigorous 3D optimization approach, will lead to a clearer and more accurate candidate trajectory for the mission.

References

[1] S. Barabash, Y. Fataana, M. Holmström, N. Krupp, M. Fränz, E. Roussos, and T. Kleine, "The apophis 2029 flyby: A unique science case for space plasma physics," *LPI Contributions*, vol. 3006, p. 2042, 2024.

[2] E. Belbruno, "Lunar capture orbits, a method of constructing earth moon trajectories and the lunar gas mission," in *19th International Electric Propulsion Conference*, p. 1054, 1987.

[3] V. Szebehely and E. Grebenikov, "Theory of orbits-the restricted problem of three bodies.," *Soviet Astronomy, Vol. 13, p. 364*, vol. 13, p. 364, 1969.

[4] D. Grebow, "Generating periodic orbits in the circular restricted three-body problem with applications to lunar south pole coverage," *MSAA Thesis, School of Aeronautics and Astronautics, Purdue University*, pp. 8–14, 2006.

[5] L. R. Irrgang, *Investigation of Transfer Trajectories to and from the Equilateral Libration Points L4 and L5 in the Earth-moon System*. PhD thesis, Master's thesis, School of Aeronautics and Astronautics, Purdue University, 2008.

[6] Jet Propulsion Laboratory, "JPL Small-Body Database." National Aeronautics and Space Administration. March 24, 2025, [online].

[7] K. C. Howell, "Families of orbits in the vicinity of the collinear libration points," *The Journal of the astronautical sciences*, vol. 49, pp. 107–125, 2001.

[8] G. Gómez, W. Koon, M. Lo, J. Marsden, J. Masdemont, and S. Ross, "Invariant manifolds, the spatial three-body problem and space mission design," in *AAS/AIAA Astrodynamics Specialist Conference*, pp. 1–20, 2001.

[9] ThrustMe, "JPT150." https://www.thrustme.fr/products/jpt150.